2012

Modeling Microalgal Abundance with Artificial Neural Networks: Demonstration of a Heuristic 'Grey-Box' to Deconvolve and Quantify Environmental Influences

David F. Millie
Palm Island Enviro-Informatics LLC., dmillie@comcast.net

Gary R. Weckman
Ohio University - Main Campus

William A. Young II
Ohio University - Main Campus

James E. Ivey
Florida Fish and Wildlife Conservation Commission

Hunter J. Carrick
Central Michigan University

See next page for additional authors

Authors
David F. Millie, Gary R. Weckman, William A. Young II, James E. Ivey, Hunter J. Carrick, and Gary L. Fahnenstiel

Environmental Modelling & Software 38 (2012) 27–39

Contents lists available at SciVerse ScienceDirect

Environmental Modelling & Software

journal homepage: www.elsevier.com/locate/envsoft

Modeling microalgal abundance with artificial neural networks: Demonstration of a heuristic 'Grey-Box' to deconvolve and quantify environmental influences

David F. Millie [a,b,c,*], Gary R. Weckman [d], William A. Young II [e], James E. Ivey [c], Hunter J. Carrick [f], Gary L. Fahnenstiel [g]

[a] Palm Island Enviro-Informatics LLC., Sarasota, FL 34232, USA
[b] Loyola University New Orleans, Department of Biological Sciences, New Orleans, LA 70118, USA
[c] Florida Fish & Wildlife Conservation Commission, Fish & Wildlife Research Institute, St. Petersburg, FL 33701, USA
[d] Ohio University, Russ College of Engineering and Technology, Department of Industrial and Systems Engineering, Athens, OH 45701, USA
[e] Ohio University, College of Business, Management Systems Department, Athens, OH 45701, USA
[f] Central Michigan University, Institute for Great Lakes Research, Mount Pleasant, MI 48559, USA
[g] National Oceanic and Atmospheric Administration, Great Lakes Environmental Research Laboratory, Lake Michigan Field Station, Muskegon, MI 49441, USA

ARTICLE INFO

Article history:
Received 4 February 2012
Accepted 10 April 2012
Available online 2 June 2012

Keywords:
Artificial intelligence
Ecological modeling
Environmental informatics
Output response surfaces
Pedagogical knowledge extraction

ABSTRACT

An artificial neural network (ANN)-based technology – a 'Grey-Box', originating the iterative selection, depiction, and quantitation of environmental relationships for modeling microalgal abundance, as chlorophyll (CHL) *a*, was developed and evaluated. Due to their robust capability for reproducing the complexities underlying chaotic, non-linear systems, ANNs have become popular for the modeling of ecosystem structure and function. However, ANNs exhibit a holistic deficiency in declarative knowledge structure (i.e. a 'black-box'). The architecture of the Grey-Box provided the benefit of the ANN modeling structure, while deconvolving the interaction of prediction potentials among environmental variables upon CHL *a*. The influences of (pairs of) predictors upon the variance and magnitude of CHL *a* were depicted via pedagogical knowledge extraction (multi-dimensional response surfaces). This afforded derivation of mathematical equations for iterative predictive outcomes of CHL *a* and together with an algorithmic expression across iterations, corrected for the lack of declarative knowledge within conventional ANNs. Importantly, the Grey-Box 'bridged the gap' between 'white-box' parametric models and black-box ANNs in terms of performance and mathematical transparency. Grey-Box formulations are relevant to ecological niche modeling, identification of biotic response(s) to stress/disturbance thresholds, and qualitative/quantitative derivation of biota-environmental relationships for incorporation within stand-alone mechanistic models projecting ecological structure.

"Ecologists … should be aware that neural networks are not just black boxes: they can open the hood, see what is in and try some trick." Scardi (2001)

1. Introduction

Artificial Neural Networks (ANNs) have become popular tools for modeling phytoplankton abundances and production/toxicity dynamics as a function of environmental 'predictors' across diverse aquatic systems (e.g. Recknagel et al., 1997; Barciela et al., 1999; Scardi and Harding, 1999; Olden, 2000; Scardi, 2001; Lee et al., 2003; Millie et al., 2006a, 2006b; Teles et al., 2006; Chan et al., 2007; Jeong et al., 2008). Briefly, ANNs are a core form of Artificial Intelligence models that discern complex associations among variables through iterative and repetitive data presentation. In essence, the correlated nonlinear patterns between 'predictor' and 'response' variables are identified, with the complex interactions reproduced and mapped. Network computations easily accommodate data of non-normal probability distributions and/or variables reflecting cyclic variation (Maier et al., 1998), traits typically observed within large 'noisy',

Abbreviations: AMB, ambient temperature; ANN, artificial neural network; BP, barometric pressure; CHL, chlorophyll; CURDIR, current direction; CURSPD, current speed; DO, dissolved oxygen; MLR, multiple linear regression; NO_x–N, nitrite/nitrate–nitrogen; PAR, photosynthetic active radiation; PE, processing elements; pH, water acidity, basicity; PRECIP, precipitation; RH, relative humidity; SAL, salinity; TEMP, water temperature; TURB, turbidity; UR–N, urea–nitrogen; WNDDIR, wind direction; WNDSPD, wind speed.

* Corresponding author. Palm Island Enviro-Informatics LLC., 4645 Stone Ridge Trail, Sarasota, FL 34232, USA. Tel.: +1 941 544 7926; fax: +1 941 378 5769.
E-mail addresses: pi_enviro@comcast.net, dmillie@comcast.net (D.F. Millie).

1364-8152/$ – see front matter © 2012 Elsevier Ltd. All rights reserved.
doi:10.1016/j.envsoft.2012.04.009

even chaotic environmental data sets (see Peck et al., 2003; Rohani et al., 2004; Murray and Conner, 2009; Wood, 2010).

ANNs typically have high-dimensional input space and do not exhibit any explicit or declarative knowledge structure. Generally, only the input-output characteristics of ANNs are of interest, with the 'knowledge' of variable relationships encoded almost incomprehensibly by synaptic weights embedded within network architecture (Fig. 1). Because of this holistic lack of model transparency, many researchers consider ANNs to be 'black-boxes' (Lek and Guegan, 1999; Olden and Jackson, 2002) and entrust a low confidence to their utilization as empirical models of ecological processes. From this, ANNs might appear to be of limited value for scientific theory generation, environmental problem solving and/or natural resource decision-making.

Aquatic scientists traditionally have relied upon multivariate linear regression (MLR) to model microalgal-environmental relationships and functionality (e.g. Cattaneo, 1987; Sarnelle, 1992; Bachmann et al., 1996, 2001; Dodds et al., 2002, 2006; Heffernan et al., 2010). Such 'white-box' parametric models are far less abstract than ANNs - the derivation of defined coefficients (based on correspondence between the response and predictor variables) affords users with a comfortable degree of model transparency. However, underlying assumptions for and/or limitations associated with MLR (e.g. requirements of a normal probability distribution and homoscedasticity for variables, inappropriate selection of predictors arising from efforts to reduce model error, strong autocorrelation among variables, etc.) restrict its 'across the board' application and may result in models without statistical merit. Moreover, a prerequisite for ecological applications of linear regression is an *a priori* knowledge of appropriate predictors for model inclusion or exclusion. In the absence of knowledge concerning the fundamental relationships of and/or interactive complexities between/among the biotic (response) and environmental (predictor) variables, MLR may result in model estimations having little or no interpretive relevance (after Millie et al., 2006a).

Accurate, reproducible prediction of system-level patterns and processes is a basic tenet of ecological forecasting. In order to provide worthwhile bases for natural resource stewardship and/or proactive mitigation of environmental disturbance/stressors, statistical-based modeling efforts require a coupling of reliable prediction with a conceptual interpretation of biotic structure and function (after Millie et al., 2006a,b, 2011). Clearly, a heuristic knowledge-extraction technique that provides exact quantitative formulations pertaining to non-linear variable interaction and prediction influences is highly desirable (c.f. Saito and Nakano, 2002). Such an approach would allow for a mathematically comprehensive, yet pragmatic understanding of environmental-biota complexity and interaction, whilst (potentially) eliminating the black-box mentality for ANNs.

The chlorophyll (CHL) *a* concentration of a water column is a universally accepted measurement of planktonic algal abundance and used to quantify community dynamics and/or growth in changing environments (Millie et al., 2010). Here, we present a network-based approach – hereafter, referred to as a 'Grey-Box' (Young and Weckman, 2009; see Oussar and Dreyfus, 2001; Johannet et al., 2007), originating the iterative selection, depiction, and quantitation of environmental variable relationships in modeling water-column CHL *a* concentrations within a coastal environment. The Grey-Box formulation: 1) was based upon knowledge extracted from a trained and validated ANN; 2) provided interpretable, multi-dimensional response surfaces depicting modeled environmental-CHL *a* relationships; and 3)

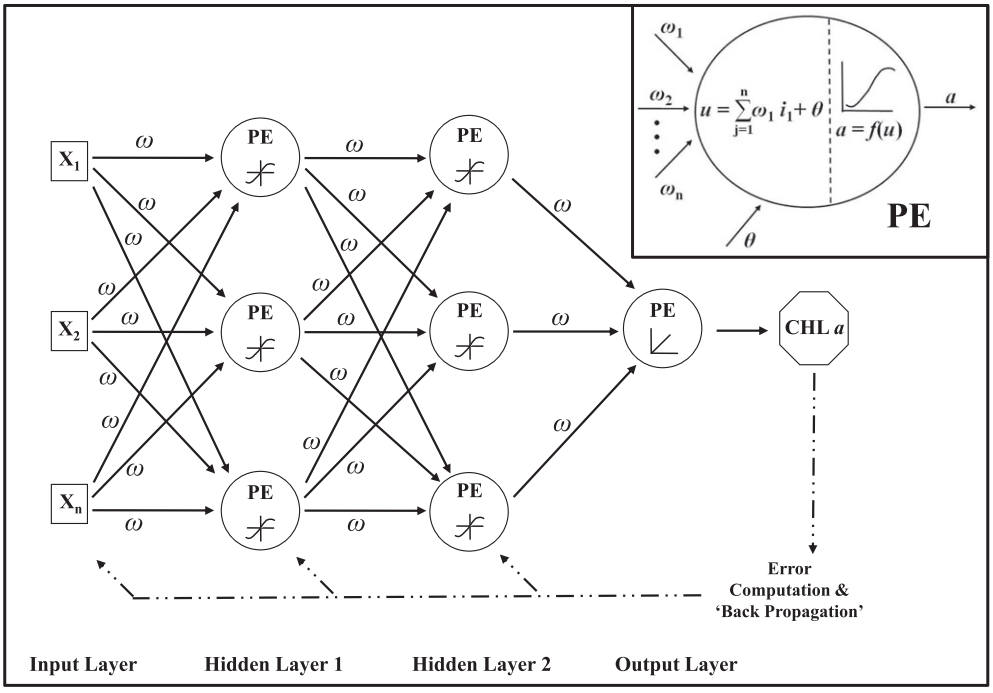

Fig. 1. Schematic of the artificial neural network (ANN) used to model chlorophyll (CHL) *a* (after Principe et al., 2000; Hu and Hwang, 2001). A feed-forward, multi-layer perceptron modeled the interaction among input variables ($x_{1\ldots n}$), synaptic weights (ω), processing elements (PEs), and CHL concentrations. The optimal network (see section 2.3) had ten and four PEs in the hidden layers one and two, respectively. Modeled and measured concentrations were compared, from which the error was computed and 'back-propagated', with the weights incrementally adjusted via a conjugate gradient learning algorithm. As error minimized with repeated data presentations, weight values stabilized and modeled concentrations increasingly approximated measured concentrations. Inset figure: Schematic depicting computational formulations of a hidden layer PE. Input values (i), whether from $x_{1\ldots n}$ or a net function from a PE, were multiplied by a synaptic weight ($\omega_{1\ldots n}$), the products summed, and combined with a bias value (θ) to produce (u) that then was transformed (via a sigmoid activation function, $f(u) = 1/(1 + e^{-u})$ to produce the output (a). Note: the PE in the output layer utilized a linear function, $f(u) = au$.

quantified environmental influences and interactions for CHL *a* through the summation of the response-surface equations.

2. Methodology

2.1. Sample site and data collection

Designated as a water body of national significance, Sarasota Bay (southwest Florida, USA) is a productive, lagoonal estuary and one of 24 systems nationwide selected to be a member of the *National Marine Estuary Program* for scientific research and education. The Bay is an excellent site with which to model phytoplankton dynamics in response to alterations in water-quality; exchange of Bay waters with Gulf of Mexico waters is limited (restricted to four narrow 'passes') and the Bay has no major freshwater tributary. As a consequence, water/nutrient inputs primarily arise from precipitation and storm-runoff events within a highly developed (residential/commercial) watershed. Such hydrological conditions result in a slightly greater salinity (SAL) – reaching 37–39 (via the Practical Salinity Scale) within Bay waters, than that of near-shore Gulf waters (ca. 35–36). Following significant rain events, SAL decreases rapidly (but not to levels of Gulf waters) and coincides with increased concentrations of non-point source terrigeneous nutrients. These conditions, in turn, impact the phytoplankton assemblage, potentially leading to altered abundances, compositional structure and holistic dominance (Ivey, unpubl. data; see Millie et al., 2004; Gilbert et al., 2006). Because of the effects of non-point source contaminants upon system-level functionality, the Bay remains listed (since 1998) by the U. S. Environmental Protection Agency as a '303d impaired' water body (FDEP, 2006).

From May to October in 2009, meteorological and hydrological data were acquired at a single site (27° 21′ 32″ N, 82° 36′ 14″ W) in the Bay via an autonomous instrument platform and a bottom-mounted Acoustic Doppler Current Profiler (Paerl et al., 2005; Millie et al., 2006a). Data for select variables (Table 1) were recorded hourly from sub-surface waters (ca. 1 m depth). Diel means of all variables were calculated and utilized for model development.

2.2. Artificial neural networks

Concentrations of CHL *a* were modeled from environmental variables using ANNs incorporating supervised training. Specifically, feed-forward multi-layer perceptrons (see Principe et al., 2000; Hu and Hwang, 2001) utilizing a back-propagation 'learning' algorithm were constructed via NeuroSolutions v6.0 software (NeuroDimension, Inc.; Gainesville, Florida USA). Predictor and modeled variables were normalized to match the range of the non-linear transfer functions in the network's hidden and output layers, respectively (Fig. 1; see Goh, 1995; Olden and Jackson, 2002).

Briefly, predictor values in each data vector (or 'exemplar') were multiplied by scalar weights prior to their summation and processing via transfer functions in hidden-layer processing elements (PEs). Values generated for hidden-layer PEs similarly were multiplied by weights and summed, prior to their processing via the transfer function in the output layer to yield a modeled CHL concentration (Fig. 1). The modeled concentration was compared to the desired measured concentration, from which the mean-square error (MSE) was computed. After presentation of all data vectors (or 'epoch'), the error was 'back-propagated' to the network and the weights incrementally adjusted, through gradient descent with momentum learning, in the direction of the minimum error among PEs (Principe et al., 2000; Olden, 2000; Lee et al., 2003). With repeated presentation of epochs, the MSE gradually minimized and modeled concentrations increasingly approximated measured concentrations.

For training, 70% of all exemplars were presented repeatedly to the network (typically 1000 to 2000 times), with 'learning'/momentum rates and step sizes allowed to vary (thereby accelerating network 'learning' and ensuring convergence to a global minimum; Barciela et al., 1999; Olden, 2000; Principe et al., 2000; Olden and Jackson, 2002). Cross-validation data (15% of all exemplars) confirmed an unbiased estimation of prediction concurrent with training. If the generated MSE within the training or cross-validation data subsets fell below 0.01 or began to increase (an indication that the network began to memorize the data; Karul et al., 2000; Gurbuz et al., 2003), training was terminated. The trained network then was applied to testing data (15% of all exemplars, not used in training and cross-validation). Data subsets for training, cross-validation, and testing were selected randomly.

A correlation coefficient denoted the agreement between modeled and measured CHL *a* concentrations. Linear regression was used to illustrate 'trend lines' for modeled:measured relationships of concentrations. An analysis of covariance tested whether slopes of regression estimations differed from the slope of a corresponding 1:1 modeled:measured relationship (SigmaPlot v12 software; Systat, Inc., Chicago, IL USA).

Table 1
Meteorological and sub-surface hydrological variables collected within Sarasota Bay.

Variable	Abbreviation (units)	Mean ± SE	Range
Ambient temperature	AMB (°C)	27.15 ± 0.18	15.94–29.48
Wind speed	WNDSPD ($m\,s^{-1}$)	4.15 ± 0.10	2.14–8.56
Wind direction	WNDDIR (compass degrees)	194.19 ± 5.34	41.90–324.76
Precipitation	PRECIP (mm)	2.6 ± 0.60	0.00–39.60
Barometric pressure	BP (Hg)	101.53 ± 0.02	100.70–102.09
Relative humidity	RH (%)	75.29 ± 0.46	53.14–88.60
Photosynthetic active radiation ($\times 10^3$)	PAR ($\mu E\,m^{-2}\,s^{-1}$).	10.24 ± 0.21	1.89–14.28
Current speed ($\times 10^{-2}$)	CURSPD ($m\,s^{-1}$)	3.30 ± 0.07	2.05–5.25
Current direction	CURDIR (compass degrees)	232.42 ± 5.80	90.44–342.02
Water temperature	TEMP (°C)	28.90 ± 0.22	20.94–31.94
Turbidity	TURB (NTU)	1.70 ± 0.06	0.35–3.90
Salinity	SAL (via the Practical Salinity Scale)	36.52 ± 0.08	35.04–38.77
Water acidity/basicity	pH ($-\log [H^+]$)	8.13 ± 0.01	7.82–8.37
Dissolved oxygen	DO ($mg\,L^{-1}$)	6.30 ± 0.06	4.91–8.20
Urea	UR-N (μM N)	3.064 ± 0.23	0.27–13.85
Chlorophyll *a*	CHL *a* ($\mu g\,L^{-1}$)	10.66 ± 0.62	1.49–35.43

2.3. Network selection

In order to identify the most optimal network for the Grey-Box model, an iterative strategy was implemented and within which diverse network architectures – inclusive of linear, sigmoid, and hyperbolic transfer functions for PEs within hidden/output layers, and diverse learning algorithms – inclusive of conjugant gradient, Levenberg-Marquardt, and momentum learning gradients, were evaluated. Initially, networks were developed and trained with the number of PEs in the first hidden layer varying by two, between two and 50, and the PEs in the second hidden layer arbitrary held to 10. The selected training algorithm was evoked using the lower bound of PEs in the first hidden layer. Twenty-five networks were trained, prior to incrementally increasing (by two, up to the maximum) the number of PEs in the first hidden layer. Resulting networks were evaluated with the network producing the least MSE within the cross-validation data set (and having optimal architecture and most efficient transfer functions/learning algorithm) chosen for further development. Using this network, the process was repeated *in toto*, with the number of PEs in the first hidden layer held to the optimal number determined in the initial training phase, the number of PEs in the second hidden layer varied by two, between two and 50. The final network architecture producing the least MSE and having the most efficient transfer functions/learning algorithm then was selected for the Grey Box formulation (Fig. 1).

2.4. Regression modeling and comparison to the ANN/Grey-Box

To compare results of the Grey-Box with that of a parametric model, a step-wise (forward) MLR model was constructed for the entire data set, as:

$$[\text{CHL } a] = \beta_0 + \beta_1 X_1 + \beta_2 X_2 + \beta_3 X_3 \cdots \beta_i X_i + \varepsilon \quad (1)$$

where $X_{1\ldots i}$ are the predictor variables, $\beta_{0\ldots i}$ are regression parameters (intercept/slopes of the regression estimation), and ε is the error (SigmaPlot v12 software).

Modeling verification statistics (root mean square error, RMSE; reliability index, RI; average error, AE; average absolute error, AAE; modeling efficiency, ME) were computed to afford direct comparison of the MLR model with the holistic ANN, and the Grey-Box model (refer to Reckhow et al., 1990; Stow et al., 2003). Briefly, the RMSE, AE, and AAE statistics denoted the generalized accuracy of performance (by quantifying differences between modeled:measured CHL concentrations), with exact agreement between modeled:measured concentrations producing a value of zero. The RI statistic signified the mean factor by which modeled CHL concentrations corresponded to measured concentrations (i.e. when modeled concentrations exactly agreed with measured concentrations, a value of one resulted). The ME statistic symbolized model prediction relative to the mean of measured CHL concentrations; a value of one signified exact similarity between modeled:measured concentrations whereas a value equal to or less than zero signified that the measured mean concentration would be no better or a better predictor that modeled value, respectively (from Stow et al., 2003).

3. Grey-Box derivation and results

Derivation of the Grey-Box utilized the most optimal ANN (section 2.3) and incorporated a step-wise (bottom-up) approach, with extraction of predictor-response information in the form of iterative, output surfaces and mathematical equations (after Young

and Weckman, 2009). Each predictor variable was permitted an opportunity to explain the variation of the response variable and presumed to explain an equal (and quantifiable) fraction of CHL *a*. Response surfaces for successive iterations accounted for progressively lesser amounts of model prediction, as:

$$[\text{CHL } a] = w_1 \cdot f(x_1, y_1) + r_1, \quad r_1 = w_2 \cdot f(x_2, y_2) + r_2, \quad r_2 = w_3 \cdot f(x_3, y_3) + r_3, \text{ and } r_{n-1} = w_n \cdot f(x_n, y_n) + r_n \tag{2}$$

where $w_{1..n}$, $f(x_{1...n}, y_{1...n})$, and $r_{1..n}$ were scaling factors, output surfaces, and iterative remainders of CHL *a*, respectively (section 3.1). In this manner, model derivation was apportioned into '*n*' iterations, each utilizing two predictor variables to explain a portion of CHL *a* (in the form of output response planes). Output surfaces then were summed as:

$$[\text{CHL}a]_{\text{Grey–Box}} = [\text{CHL}a]_{1\text{st iteration}} + [\text{CHL}a]_{2\text{nd iteration}\ldots} + [\text{CHL}a]_{n\text{th iteration}} + r_n \tag{3}$$

3.1. Iterative response surfaces

3.1.1. Initial iteration

The initial output surface, $f(x_1, y_1)$, was postulated to represent the majority of variation within CHL *a*. Originally, ANNs incorporating 15 candidate predictor variables were developed, trained, and tested. The slope of the modeled:measured regression for the 'most optimal' network (Fig. 2A) did not differ from a corresponding 1:1 relationship. Following this, a sensitivity analysis ($S_{1...n}$) provided an approximate measure of the relative importance for predictor variables upon CHL *a* concentrations (Fig. 2B). Specifically, each predictor was altered (plus/minus two standard deviations about the mean, 50 steps-per-side), while other predictors remained fixed at their respective means (Principe et al., 2000). In this manner, approximately 95% of the data range for each predictor variable was incorporated into the analysis and reduced the likelihood that extreme data outliers would bias the outcome (Jeong et al., 2003).

Pertinent network information (i.e. input-hidden-output layer architecture, weights, biases, transfer-threshold functions) was

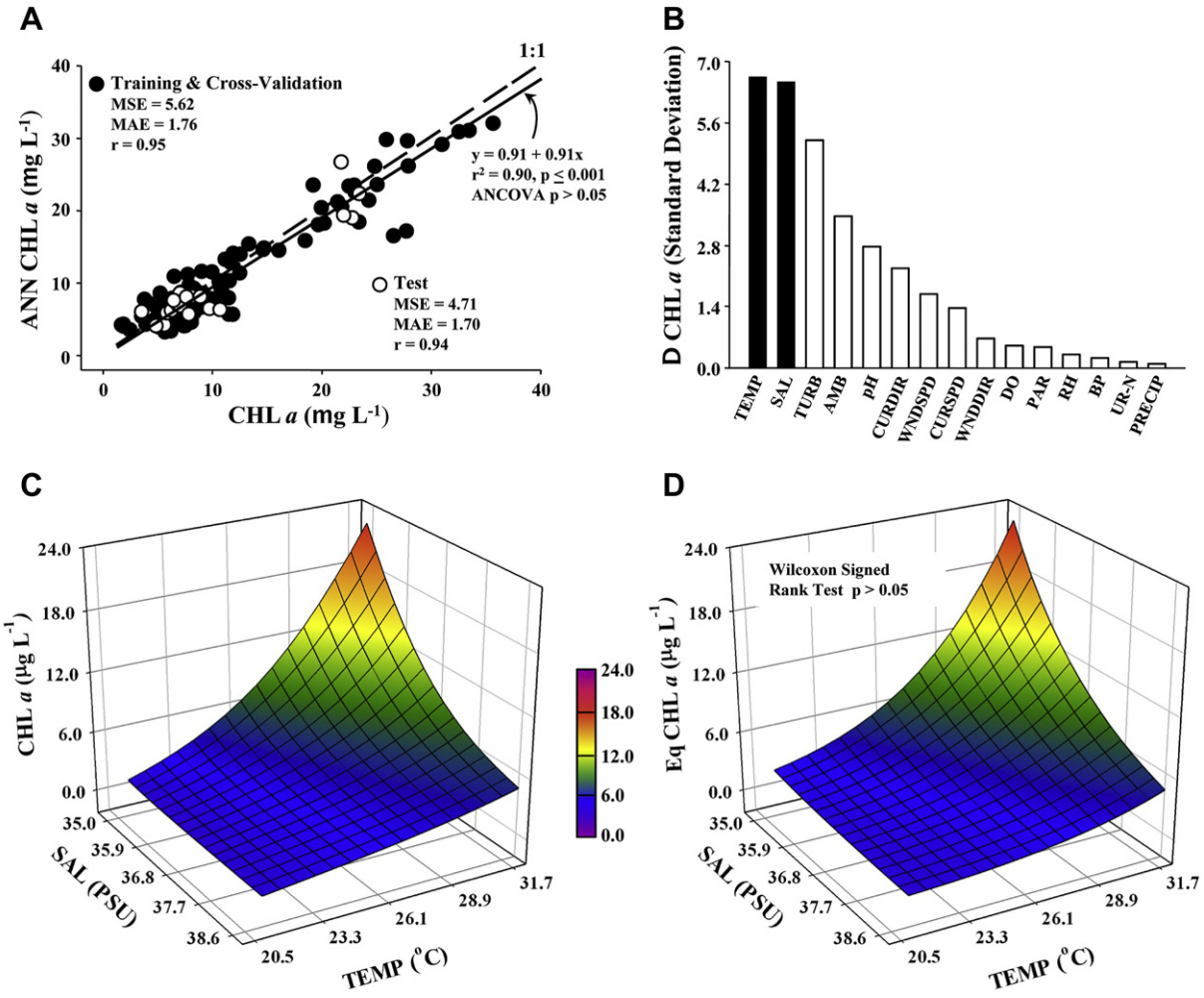

Fig. 2. A) Modeled CHL *a* concentrations as a function of measured concentrations for the 'holistic' artificial neural network (ANN) (i.e. iteration one; see section 3.1.1). The dashed line represents a 'desired' 1:1 relationship. The solid line and corresponding statistical information represents a 'best fit' for the modeled:measured relationship, as derived from linear regression. B) Results of a sensitivity analysis across ± one SD variation performed on the training data. Black-filled bars indicate variables selected for development of the subsequent iterative response surface. C) Response surface (generated via the ANN) for CHL as a function of TEMP and SAL, varied across their data ranges. Values for other predictors held to their respective sample means. D) Response surface (generated via a 'Power B' equation) for CHL as a function of TEMP and SAL, varied across their data ranges. Corresponding statistical information denotes similarity to the ANN-derived response plane as a function of *x*, *y* variable pairs.

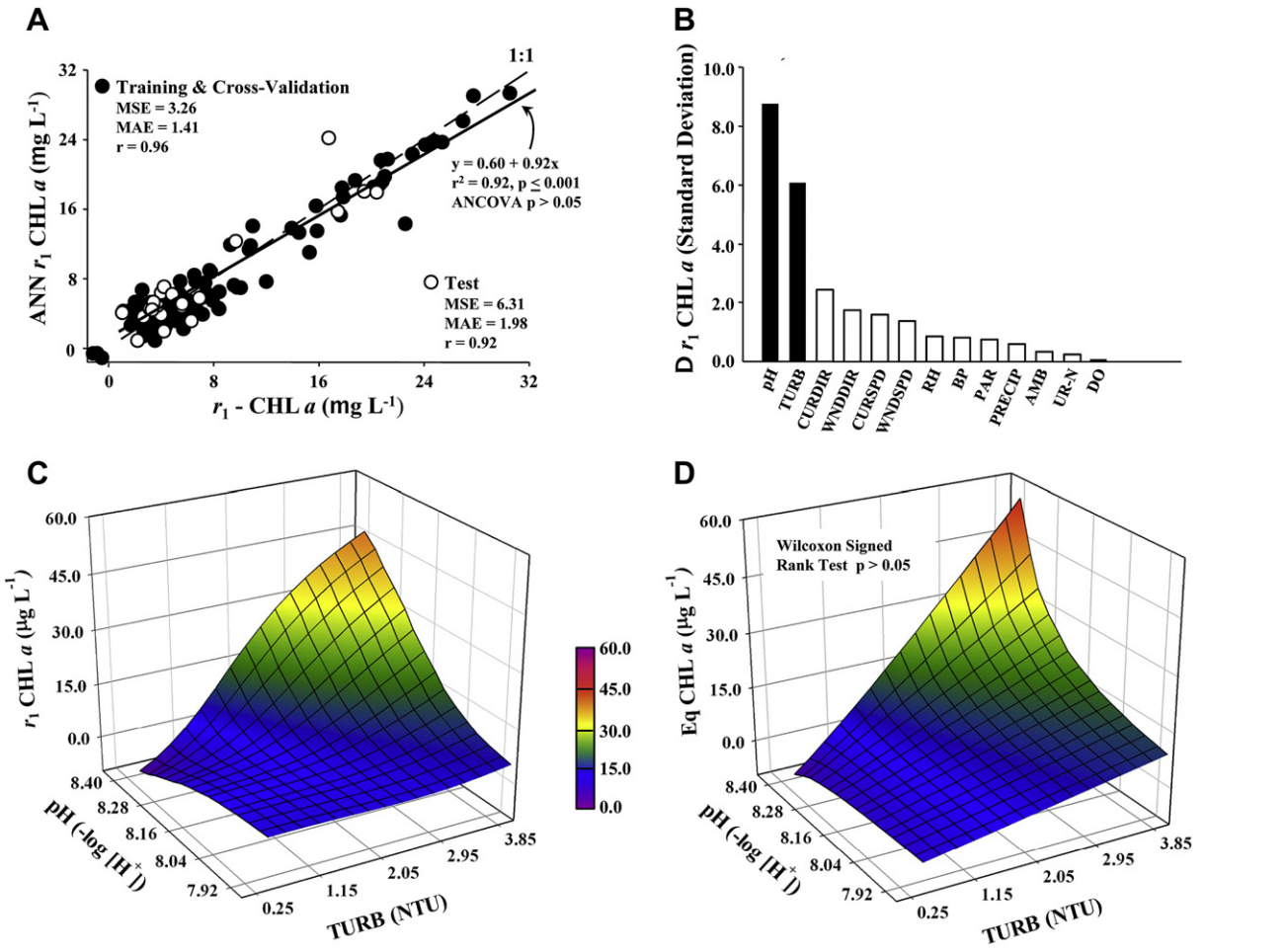

Fig. 3. A) Modeled concentrations as a function of measured concentrations for the artificial neural network (ANN) modeling r_1 CHL *a* (i.e. iteration two; see section 3.1.2). B) Results of a sensitivity analysis across ± one SD variation performed on the training data. Black-filled bars indicate variables selected for development of the subsequent iterative response surface. C) Response surface (generated via the ANN) for r_1 CHL as a function of pH and TURB, varied across their data ranges. Values for other predictors held to their respective sample means. D) Response surface generated via a 'Rational C' equation for r_1 CHL as a function of pH and TURB, varied across their data ranges. Lines and statistical information as in Fig. 2.

incorporated into Excel ver. 2010 spreadsheet software (Microsoft Corp.; Seattle, WA USA). Based upon results of the initial sensitivity analysis, water temperature (TEMP) and SAL were the two predictors having the greatest impact upon CHL *a* and chosen to create $f(x_1, y_1)$. Within the ANN, TEMP and SAL were varied between their respective minimum- maximum data ranges (with values for other predictors held to their sample means – a procedure similar to that of a sensitivity analysis) and from which, a three-dimensional response surface for CHL *a* was generated (Fig. 2C).

Next, a trial-and-error procedure to fit a planar equation to the modeled response surface was undertaken. Fifteen distinct mathematical expressions, inclusive of power, polynomial, rational, sigmoid, and Taylor series equations, were examined. The response surface generated by a 'Power B' equation was equivalent to the modeled response ($p > 0.05$; Fig. 2D), as determined by a Wilcoxon Signed Rank Test assessing CHL concentrations as a function of *x*,*y* variable pairs. (Note: concentrations of all network- and equation-derived surfaces were neither normally distributed nor displayed equal variances, thereby necessitating non-parametric comparisons). A Generalized Reduced Gradient nonlinear programming algorithm (GRG2; Lasdon et al., 1978) optimized the constant (a) and variable factors (b, c, d) for the 'Power B' equation, as:

$$[\text{CHL } a_{1\text{st iteration}}] = a + b\left(x_1^c * y_1^d\right), \text{ or}$$

$$[\text{CHL } a_{1\text{st iteration}}] = 1.16 + 5.0\exp + 17\left(\text{TEMP}^{6.59} * \text{SAL}^{-17.01}\right) \quad (4)$$

A scaling factor ($w_{i\ldots n}$) for the response plane then was calculated. Specifically, factors were determined as the relative summation for the two variables having the greatest impact upon the modeled variable (determined via sensitivity scores), as:

$$w_m = \frac{S_m(x_m) + S_m(y_m)}{\sum_{i=m}^{n} S_i(x_i) + \sum_{i=m}^{n} S_i(y_i)} \cdot \left(1 - \sum_{i=1}^{n-1} w_i\right), \text{ or}$$
$$w_1 = \frac{S_1(\text{TEMP}) + S_1(\text{SAL})}{S_1(\text{TEMP}) + S_1(\text{SAL}) + \cdots S_i(y_i)} \cdot (1 - 0) = 0.41 \quad (5)$$

Importantly, the generalized form for the scaling expression required that calculated factors sum to one. Because w_1 represents the scaling factor for the initial response surface, there were no previous factors to consider; as such, its calculation included a multiplicand of one (i.e. 1–0). From Eq. (2), the mathematical expression for the first iteration became:

$$\text{CHL } a_{1\text{st Iteration}} = 0.41 \cdot \left(1.16 + 5.0\exp 17\left(\text{TEMP}^{6.59} \cdot \text{SAL}^{-17.01}\right)\right. \quad (6)$$

3.1.2. Subsequent iterations

A second iteration was undertaken to deconvolve (in part) the remaining 'unexplained' variation (r_1) between CHL *a* concentrations and the scaled response surface of the initial iteration (Eq. (2)). It first was necessary to correct the response variable in each data vector for the amount of variation accounted for by the initial response surface (from Eq. (5)), as:

$$r_1 = [\text{CHL } a_{1\cdots n}] - (f(x_1, y_1)\cdot w_1) \tag{7}$$

The ANN training/testing strategy (Section 2.2) was repeated, incorporating 13 predictor variables to model r_1 (Fig. 3A; note: the variables, TEMP and SAL, utilized for the response surface of the first iteration were eliminated from consideration). The slope of the modeled:measured regression for the network did not differ from a corresponding 1:1 relationship. A sensitivity analysis for the second trained network (S_2) identified water acidity/basicity (pH) and turbidity (TURB) as the variables having the greatest impact upon modeled r_1 (Fig. 3B). These two variables then were used to create a second modeled response surface, $f(x_2, y_2)$ (Fig. 3C). The response surface produced from a 'Rational C' equation (Fig. 3D) was similar ($p > 0.05$) to the modeled surface. The GRG2 algorithm determined the appropriate equation constants/factors and the scaling factor for the response surface (w_2) was calculated (taking into account the aforementioned requirement that the derived scaling factors for iterations sum to one), as:

$$w_2 = \frac{S_2(\text{pH}) + S_2(\text{TURB})}{S_2(\text{pH}) + S_2(\text{TURB}) + \cdots S_2(x_n) + S_2(y_n)}\cdot(1 - w_1) \tag{8}$$

The mathematical expression for the second iteration then became:

$$[\text{CHL } a_{2\text{nd Iteration}}] = 0.35\cdot\left(\frac{(0.72 - 0.01{*}\text{pH} + 0.115{*}\text{TURB})}{(1 - 1.08{*}\log_{10}\text{pH} + e{*}\log_{10}\text{TURB})}\right) \tag{9}$$

Succeeding iterations continued to deconvolve the remaining variation in CHL *a* left unexplained by the response surfaces of previous iterations (see Eq. (2)). Prior to modeling, respective iterative remainders for use in the third and fourth iterations (r_2 and r_3, respectively) were corrected for the amount of variation explained by the response surface(s) within the preceding iteration(s), as:

$$r_2 = r_1 - (f(x_2, y_2)\cdot w_2), \text{ and } r_3 = r_2 - (f(x_3, y_3)\cdot w_3) \tag{10}$$

Network training/testing (Fig. 4A and B) for the third and fourth iterations used 11 and nine predictor variables, respectively, after successive removal of pairs of predictors used in previous iterations. For ANNs modeling r_2 and r_3, the slope of the modeled:measured regression differed from a corresponding 1:1 relationship. Sensitivity analyses identified photosynthetic active

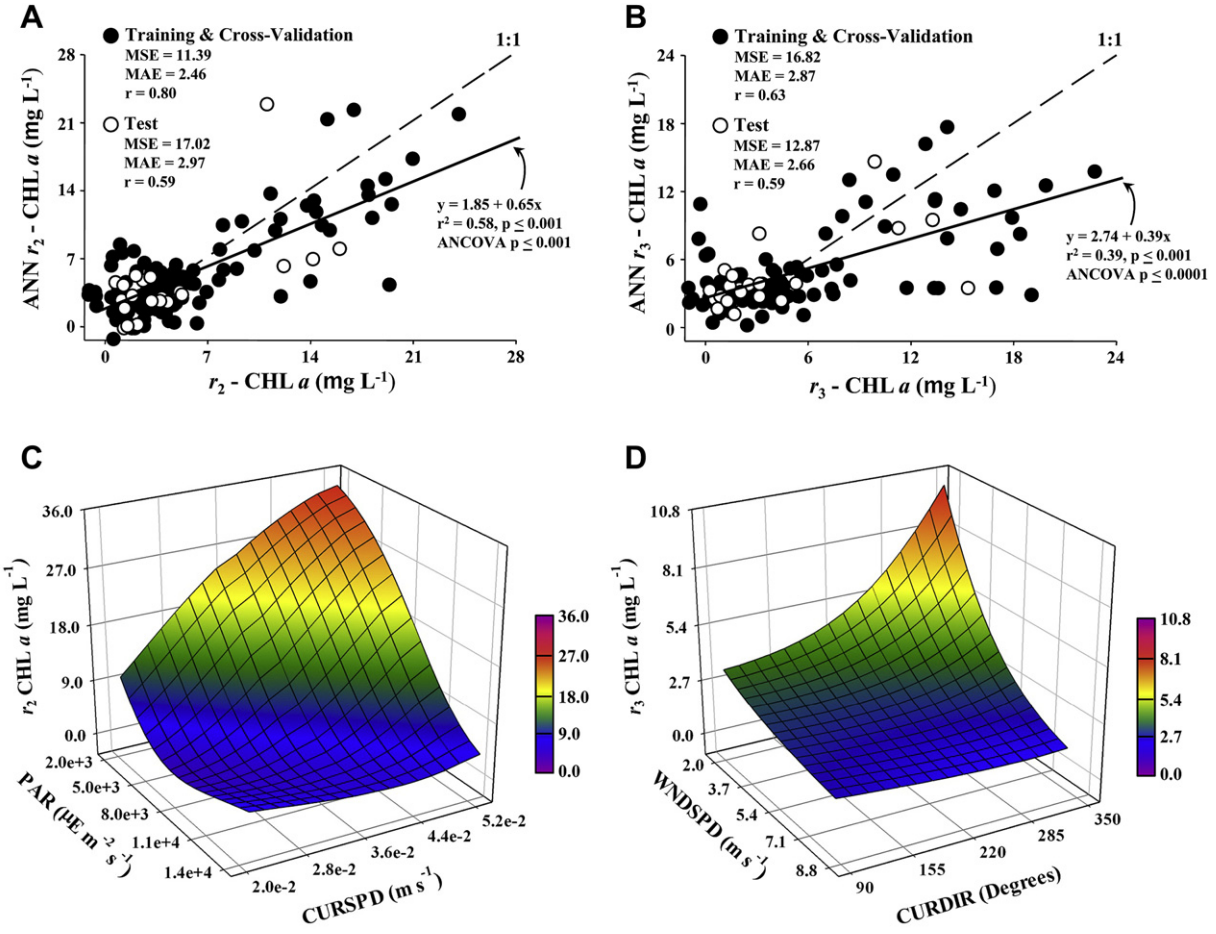

Fig. 4. A & B) Modeled concentrations as a function of measured concentrations for the artificial neural network (ANN) modeling (A) r_2 CHL *a* and (B) r_3 CHL *a* (i.e. iterations three and four; see section 3.1.2). Lines and statistical information as in previous figures. C & D) ANN-derived response surfaces for (C) r_2 CHL *a* as a function of PAR and CURSPD, varied across their data ranges and (D) r_2 CHL *a* (generated via the ANN) as a function of WNDSPD and CURDIR, varied across their data ranges. Accompanying sensitivity analyses and equation-derived response planes not shown (for details, see section 3.1.2).

radiation (PAR) and current speed (CURSPD), as (x_3, y_3), and wind speed (WNDSPD) and current direction (CURDIR), as (x_4, y_4), to have the greatest impact upon modeled r_2 and r_3, respectively (data not shown). These variables then were used to create the response surfaces, $f(x_3, y_3)$ and $f(x_4, y_4)$ (Fig. 4C and D, respectively). Response surfaces created from 'Rational B' equations were identical ($p > 0.05$) to modeled surfaces for both the third and fourth iterations. Scaling factors then were calculated, again taking into account the requirement that derived factors for all iterations sum to one. Mathematical expressions for the third and fourth iterations became:

$$[\text{CHL } a_{3\text{rd Iteration}}] = 0.12 \bullet \frac{(70.89 + 12.69{*}\log_{10}\text{CURSPD} - 12.37{*}\log_{10}\text{PAR})}{(1 - 13.43{*}\text{CURSPD} + 0.01{*}\text{PAR})}, \text{ and}$$
$$[\text{Chl } a_{4\text{th Iteration}}] = 0.06 \cdot \frac{(8.01 - 1.98{*}\log_{10}\text{CURDIR} - 2.69{*}\log_{10}\text{WNDSPD})}{(1 - 0.01{*}\text{CURDIR} + 0.03{*}\text{WNDSPD})} \quad (11)$$

After four iterations, cumulative improvements (i.e. decreases) in error metrics for networks of training/cross-validation datasets had lessened (Table 2). Importantly, the value of the scaling factor for the fourth iteration was small (0.06), having been sequentially reduced from 0.41 to 0.35, to 0.12 in the first, second, and third iterations, respectively). Also, determination coefficients for modeled:measured comparisons of cumulative iterative networks had maximized (to ca. 0.75). As such, additional iterations were deemed unnecessary.

3.2. Grey-Box rotation and offset

To depict the amount of CHL accounted for by successive iterations, response surface equations for modeled concentrations were plotted cumulatively as a function of measured concentrations. Specifically, the plot (Fig. 5A) for the first iteration was constructed from Eq. (6), incorporating the predictor variables, TEMP and SAL. The plot following the second iteration (Fig. 5B) arose from the cumulative contribution of Eqs. (6) and (9), incorporating the variables, pH and TURB. Subsequent plots were derived incorporating the cumulative contributions of iteration three with variables, CURSPD and PAR, and iteration four with variables, CURDIR and WNDSPD (Eq. (11); Fig. 5C and D).

The final cumulative plot then was 'rotated' and 'offset', whereby the summation of the scaled estimates was 'centered' via the GRG2 algorithm onto measured CHL concentrations within the training and cross-validation datasets (Fig. 6):

$$[\text{CHL } a_{\text{Grey-Box}}] = a + b([\text{CHL } a_{\text{iteration }1}] + [\text{CHL } a_{\text{iteration }2}]\cdots + [\text{CHL } a_{\text{iteration }n}]) \quad (12)$$

where a and b represented the equation constant (y-intercept) and slope, respectively. Successive iterations of the algorithm sought to minimize the sum of squares of the differences between plotted and measured values. Initially, the algorithm utilized values of zero and one for a and b, respectively, and quadratic extrapolation, after which a conjugate search method and a central differencing technique calculated the derivative for each iteration. The final, rotated and offset Grey-Box became:

$$[\text{CHL } a_{\text{Grey-Box}} = -13.3 + 2.25\left(\begin{array}{c}(0.41{*}1.16 + 5.0\text{E}17{*}(\text{TEMP}^{6.592}{*}\text{SAL}^{-17.01})) \\ + \left(0.35{*}\frac{(0.72 - 0.01{*}\text{pH} + 0.115{*}\text{TURB})}{(1 - 1.08{*}\log_{10}\text{pH} + e{*}\log_{10}\text{TURB})}\right) \\ + \left(0.12{*}\frac{(70.89 + 12.69{*}\log_{10}\text{CURSPD} - 12.37{*}\log_{10}\text{PAR})}{(1 - 13.43{*}\text{CURSPD} + 0.01{*}\text{PAR})}\right) \\ + \left(0.06{*}\frac{(8.01 - 1.98{*}\log_{10}\text{CURDIR} - 2.69{*}\log_{10}\text{WNDSPD})}{(1 - 0.01{*}\text{CURDIR} + 0.03{*}\text{WNDSPD})}\right)\end{array}\right) \quad (13)$$

Table 2
Error metrics (SSE, sum of squares; MSE, Mean square error; MAE, mean absolute error) and determination coefficients (r^2), derived via regression of modeled against measured chlorophyll concentrations for the holistic artificial neural network (ANN) and the Grey-Box model. Iterative data represent cumulative contributions of iterative surface equations (using appropriate predictor variables) in successive iterations (see sections 3.1.1 and 3.1.2).

Data set	Metric	Iteration 1	Iteration 2	Iteration 3	Iteration 4	Grey Box	ANN
Training and cross validation	SSE	13092.62	6807.35	5874.57	5573.30	1736.40	679.37
	MSE	108.20	56.26	48.55	46.06	14.35	5.62
	MAE	7.86	5.27	4.83	4.67	2.93	1.76
	RSQ	0.35	0.74	0.74	0.75	0.75	0.90
Test	SSE	1739.17	848.33	712.32	672.62	178.07	98.91
	MSE	82.82	40.40	33.92	32.03	8.48	4.71
	MAE	6.99	4.53	3.91	3.71	2.25	1.70
	RSQ	0.25	0.79	0.79	0.79	0.77	0.88

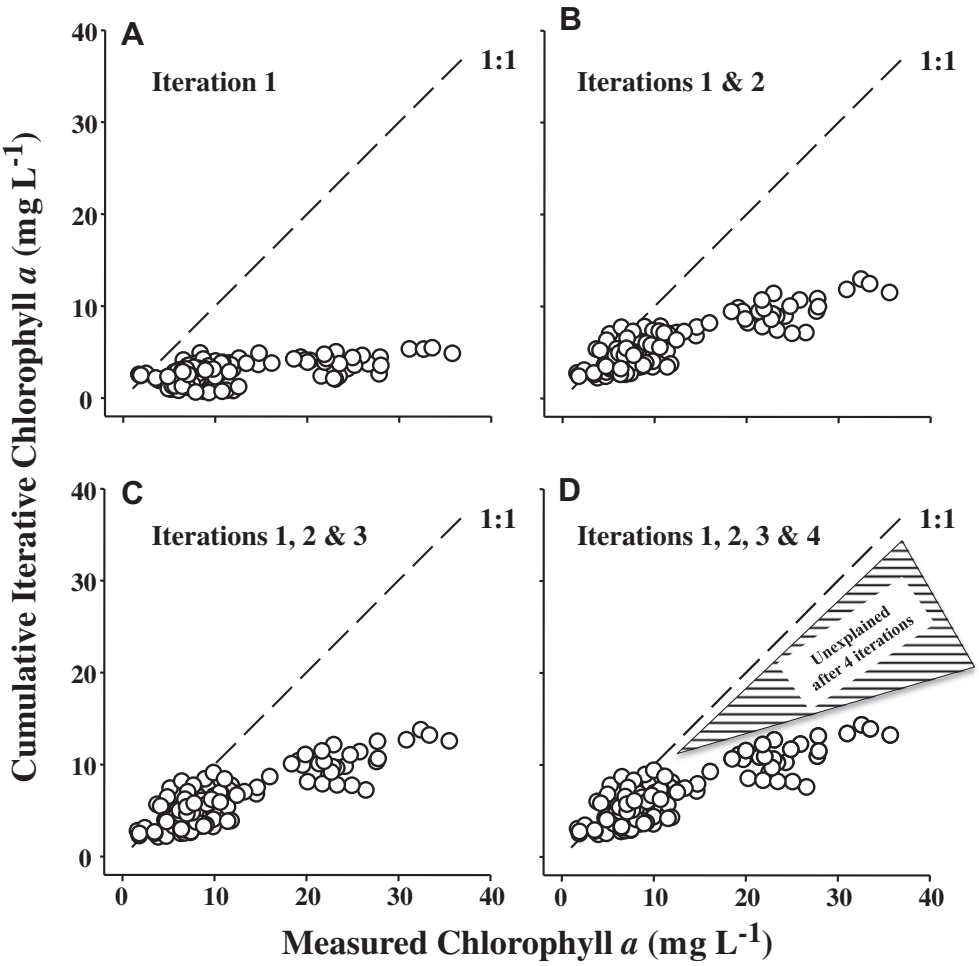

Fig. 5. Cumulative concentrations of CHL *a* accounted for by planar surface equations (using appropriate predictor variables) in successive iterations as a function of measured concentrations (see sections 3.1.1 and 3.1.2). A) 'Power B' equation, using the predictors, SAL/TEMP (Eq. (12)); B) 'Power B' and 'Rational C' equations using the predictors, SAL/TEMP and pH/TURB, respectively; C) 'Power B', 'Rational C', and 'Rational B' equations using the predictors, SAL/TEMP and pH/TURB, and PAR/CURSPD, respectively; D) 'Power B', 'Rational C', 'Rational B' and 'Rational B' equations using the predictors, SAL/TEMP, pH/TURB, PAR/CURSPD, and WNDSPD/CURDIR, respectively. The dashed line represents a 'desired' 1:1 relationship. The 'pie-shaped wedge' represents the amount of variation in CHL *a* left 'unexplained' after four iterations due to the use of only eight (of the potential 15) predictor variables and that attributable to autocorrelation among all predictors.

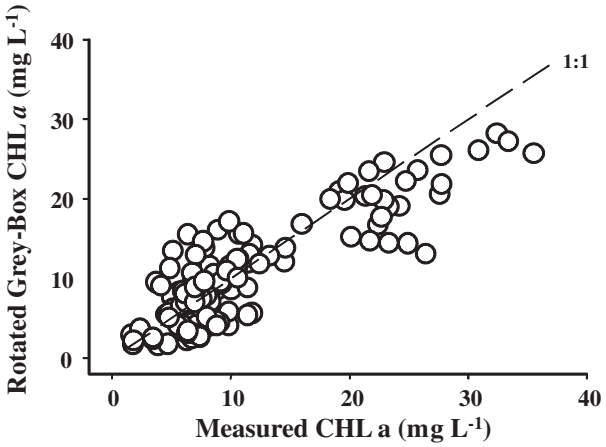

Fig. 6. Cumulative concentrations of CHL *a* accounted for by planar surface equations following four successive iterations (Fig. 5D), and 'rotation' and 'offset' as a function of measured concentrations. For 'rotation', the summation of the scaled estimates was 'centered' via the GRG2 algorithm onto measured concentrations (see section 3.2). The dashed line represents a 'desired' 1:1 relationship.

3.3. MLR and comparison to the ANN and Grey-Box

The forward-stepwise MLR model selected a linear combination of six variables to estimate CHL *a* concentrations ($r^2_{adj} = 0.65$, $n = 142$, $p \leq 0.001$) as:

$$[\text{CHL } a] = 44.408 + (3.44*\text{TURB}) - (1.93*\text{SAL}) + (1.11*\text{TEMP}) + (377.86*\text{CurSpd}) - (1.72*\text{WndSpd}) - (0.001*\text{PAR}) \quad (14)$$

Interestingly, the six predictor variables selected for the stepwise MLR also were utilized (of eight variables total) within the derivation of the Grey Box model. Although the errors of the predictor coefficients were normally distributed around the regression estimate (as determined by a Shapiro–Wilks test, $p = 0.96$) and modeled residuals were independent (as determined by the Durbin–Watson statistic > 2), the dependent variable (CHL *a*) displayed a non-normal distribution and heteroscedasticity ($p = <0.001$, as determined by a Spearman rank correlation test

between residual and measured concentrations). A scatter plot of model residuals as a function of predicted CHL a concentrations (data not shown) depicted asymmetry around the 'zero line', thereby signifying a condition of nonlinearity.

Non-linear transformations (e.g. square/fourth-root, logarithmic) were applied to the data distributions in attempts to stabilize the variance. Although logarithmic transformation of the dependent variable provided for homoscedasticity of CHL *a* ($p = 0.84$), MLR models incorporating transformed variables performed (only) as equally or underperformed the regression model utilizing non-transformed variables ($r^2 \approx 0.60$, $p \leq 0.001$; models not shown), whilst failing the test for normality of predictor coefficients about the regression ($p < 0.001$).

Based upon model verification statistics (Table 3), the holistic ANN and the Grey-Box clearly outperformed the MLR. Values for RMSE, RI and AAE were greatest for the parametric model, with corresponding values for the Grey-Box between that of the MLR model and the holistic ANN. Conversely, the greatest and least ME values occurred for the ANN and the MLR model, respectively, denoting these models to have the greatest and least efficiency in modeling (i.e. agreement between modeled:measured concentrations). Although AE similarly is a measure of prediction accuracy, values for all models approximated zero. Stow et al. (2003) stated that such AE values "…can be misleading because negative and positive discrepancies can cancel each other…", indicating that RMSE and AAE are more interpretable statistics because they "…accommodate the shortcoming of the average error by considering the magnitude rather than the direction of each discrepancy."

4. Discussion

Considered to be universal approximators capable of learning any deterministic function (Horkik et al., 1989), the multilayer feed-forward networks utilized for the Grey-Box model provided a systematic 'bottom-up' estimation of microalgal abundance from select environmental predictors. With this approach, the iterative complexity of prediction potentials among candidate predictors was deconvolved and by means of pedagogical knowledge extraction (i.e. the output surfaces), the step-wise effects of (pairs of) predictors upon the intrinsic variance and magnitude of CHL *a* dynamics were depicted. Importantly, this approach afforded comprehensible quantitative translations (via discrete mathematical equations) for iterative predictive outcomes, as well as a set of algorithmic rules across iterations.

The Grey-Box initiated with empiricism, yet moved towards a semi-analytical formulation. The sensitivity analysis for the holistic ANN (utilizing all candidate predictors) denoted SAL and TEMP to be the variables having the greatest influence upon CHL *a*. The subsequent response surface depicted a curvilinear relationship between CHL *a* concentrations and these 'most sensitive' predictors, with the greatest concentrations occurring at the lower and upper data ranges for SAL and TEMP, respectively. Such relationships were intuitive; the 'wet' season in tropical-temperate south Florida extends from May to October (the time period during which water quality data was collected in Sarasota Bay) and is typified by heightened PRECIP, resulting in the introduction of nutrient-enriched, freshwater inflows from the adjacent watersheds into brackish coastal waters. Reflecting the increased metabolic activity and resource utilization by phytoplankton to greater TEMPs and nutrient enrichment, CHL *a* concentrations in Florida's estuarine waters often are greatest during warm, summer months (e.g. Millie et al., 2004). For such a seasonal relationship in Sarasota Bay, a mathematical expression that suitably accounted for the magnitude and dynamics in CHL *a* as a function of SAL and TEMP was formulated. Subsequent iterations selected predictor variables known to influence (or be influenced by) phytoplankton biomass/production (PAR, pH, TURB) and variables (WNDSPD, WNDDIR, CURDIR) denoting physical forcing factors that impact (localized) near-surface biomass accumulations (Paerl, 1988; Paerl et al., 1998; Millie et al., 2009, 2010). From the CHL response surfaces incorporating these (pairs of) predictor variables, mathematical expressions also were derived.

An initial premise for Grey-Box derivation was that environmental predictors were permitted equal opportunities to explain the variation in CHL concentrations. The number of predictor variables available for network training/validation decreased (in pairs) with successive iterations. Accordingly, scaling factors for response surfaces were derived (via sensitivity analyses) to account for the lesser amount of CHL *a* attributable to predictors in subsequent iterations. Intuitively, absolute values of $w_{i\ldots n}$ would decrease as the number of response surfaces increased. The lesser amount of model prediction accounted for by progressive iterations was illustrated by the increasing 'lack of fit' (i.e. increased scatter) between modeled:measured CHL concentrations and the departures from a 1:1 modeled:measured relationship within the third and fourth iterations (refer to Fig. 4). The iterative adjustment of the CHL concentrations accompanying the decreasing number of predictors continually afforded the most sensitive predictors to have the greatest predictive influence and thereby, progressively improved upon model prediction. If a scaling factor had not been utilized, the surface equation generated for the first iteration would have 'over fit' the data, and not allowed predictor variables in subsequent iterations to holistically account for the 'reddened' (i.e. acute/chronic variability) and 'white' (natural variability) noises in CHL *a* data left unexplained as iterative remainders (see Rohani et al., 2004). In founding the scaling factor upon sensitivity analysis, it also must remembered that it is possible for only one (or a few) predictors to significantly impact the response variable (i.e. a sensitivity an order of magnitude greater than other candidate predictors). In such instances, the derived scaling factor(s) from the opening iterations would provide for the remaining predictors (i.e. surfaces) to explain an insignificant fraction of the response variable. In contrast, if all variables were holistically identical in terms of their impact upon CHL concentrations (i.e. a relative equal sensitivity for predictors), nearly equivalent-scaling factors would result, with the response variable explained equally well by successive output surfaces.

Not surprisingly, a diminishing return in terms of prediction occurred with the reduction of variable pairs from the pool of potential predictors in progressive iterations. To illustrate this, CHL *a* concentrations for the training and cross-validations data sets were sorted in order of ascending values and plotted (cumulatively for successive iterations) as a function of modeled values (Fig. 7). The initial scaled surface incorporating the predictors, SAL and TEMP, contributed the majority (albeit somewhat a dynamic proportion) of relative prediction throughout the range of the modeled response. Relative estimations arising from the second (iterative) scaled surface increased disproportionately with

Table 3
Model verification statistics – root mean square error (RMSE), reliability index (RI), average error (AE), average absolute error (AAE), and modeling efficiency (ME) for direct comparison of parametric multiple linear regression (MLR), the holistic artificial neural network (ANN), and the Grey-Box model (refer to sections 2.4 and 3.3).

Model type	Statistic				
	RMSE	RI	AE	AAE	ME
MLR	4.23	1.90	−0.02	3.34	0.67
ANN	2.34	1.34	−0.05	1.74	0.90
Grey-Box	3.66	1.50	0.00	2.83	0.75

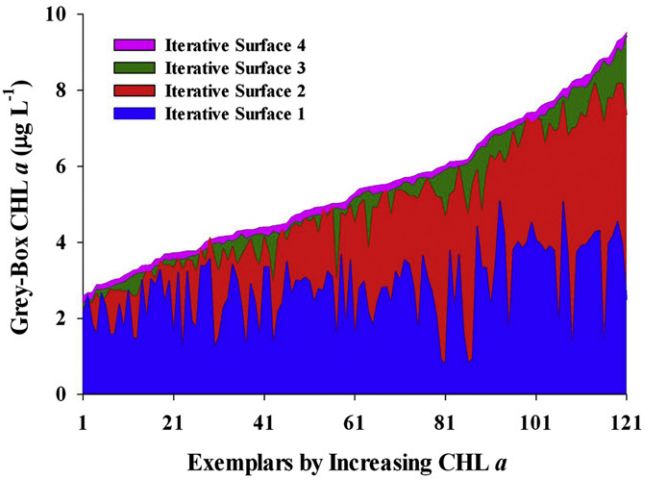

Fig. 7. Cumulative contribution of iterative equations within the estimated Grey-Box model across the range of measured CHL concentrations for the training and cross-validation data subsets. The one hundred twenty-one concentrations (i.e. 'exemplars', see section 2.2) were sorted from least to greatest and numbered in increasing value to denote differential impacts of scaled equations upon model prediction across the range of measured concentrations.

measured concentrations, denoting a nonlinear relationship evidenced by slight contributions at lesser concentrations and significant contributions at the greatest concentrations. From this, SAL and TEMP appeared to provide the principal and most consistent prediction across lesser CHL concentrations, whereas pH and TURB were primary predictors for the greatest concentrations (also demonstrated by the differences in the scaling of the *y*-axes in Figs. 2C/D and 3C/D). The third and fourth iterations continued to improve upon model performance (in terms of the model error); however, the relative contribution of the selected predictors for these iterations to model prediction was minimal.

Although successive iterations of the Grey-Box improved model performance - in both the training/cross-validation and testing data sets, maximum values for the determination coefficient between modeled:measured values were reached by the second iteration (i.e. after inclusion of four predictor variables in the model). It must be remembered that the coefficient of determination is a metric denoting the proportion of the response variation explained by regressors in a model for a conditional probability distribution, or 'what is the value of a response variable, *y*, given a specific value of the variable *x*, with the distribution parameters, θ'; ($P(x|y, \theta)$. For environmental data sets, response and predictor variables should be considered as multivariates in a joint probability distribution, or 'what is probability of two or more things (*y* and single/multiple *x*) happening together'; $P(x,y|\theta)$. Accordingly, the determination coefficient alone would not adequately describe the complexity of predictor/response relationships and it would be more appropriate to utilize error metrics and scaling factors for evaluating model performance between successive iterations. Such was the case for the third iteration of both the training/cross-validation and testing data sets, when coefficient values for the fitted equation decreased only slightly (from that of the second iteration), but error metrics and values of $w_{i\ldots n}$ continued to improve (i.e. decrease). A fifth iteration (data not shown), in which urea nitrogen (UR-N) and dissolved oxygen (DO) were selected as predictor variables, did not improve significantly upon the (cumulative) results following the fourth iteration; relative improvements in values of *w* (from 0.06 to 0.04) and model error (from 46.06 to 44.44 MSE and 5573 to 5377 SSE) were relatively minimal. Accordingly, this fifth iteration was deemed unnecessary and only four iterations were included in the Grey-Box model.

The predictive accuracy of the Grey-Box clearly was related to the non-linear optimization methodology chosen to derive the 'best fit' mathematical expressions for the iterative surfaces of response/predictor variables. The GRG2 algorithm utilized to derive equation constants and factors is a gradient-descent approach known for its robustness and reliability. However, Gill et al. (1981) questioned whether the GRG2 algorithm truly reaches a global optimum in nonlinear problems, whereby errors in the gradient descent affect performance. In addition, although all 'best fit' equations suitably addressed the generated (and relatively simple) curvilinear output surfaces within this demonstration, more complex response surfaces likely would require a specialized optimization technique (e.g. the Levenberg–Marquardt nonlinear least squares fitting algorithm; see Moré, 1978). Similarly, the selection of equations for the mathematical generalization of output surfaces was limited to power, polynomial, and rational representations. For instances where highly developed output surfaces are generated, different and more sophisticated surface equations should be considered.

Traditional sensitivity about-the-mean analysis (i.e. noting the variation in model output attributable to deviations of individual input variables across their sample range, while other inputs are held to their respective sample means) was used to extract the 'cause and effect' relationships between predictor variables and the modeled CHL *a* concentrations. Sensitivity analysis was chosen for this demonstration due to the ease in its computation, the simplicity of its comprehension, and its universal application within statistical/mechanistic modeling (Saltelli et al., 2004; Yeung et al., 2010). Importantly, the use of sensitivity analysis afforded a systematic means to exclude input variables from the Grey-Box that did not contribute significantly to overall prediction, thereby reducing model complexity and improving model quality (Weckman et al., 2009). Complementary, yet more complex methods for determining variable influences and/or decision utilities from networks do exist (see Gevery et al., 2003; Olden et al., 2004; Weckman et al., 2005, 2009) and might have been utilized for the derivation of the Grey-Box model. Nonetheless, from whichever methodology utilized, the selection of input variables and the derivation of scaling factors for successive Grey-Box iterations requires quantifiable rankings of predictive importance for model inputs.

The ANN and Grey-Box models outperformed MLR, proving to be an attractive substitute (to parametric linear models) for identifying environmental influences upon CHL *a* within Sarasota Bay. This greater performance is not surprising. In theory, an ANN encompasses linear regression and due to the introduction of a model architecture suited for reproducing the non-linear, complexities/dynamics of a biotic response to environmental forcing (see Sugihara et al., 1990; Austin, 2002; Oksanen and Minchinb, 2002), should perform as well, or better than MLR models (Gonzalez, 2000). However, one should not solely focus on whether MLR appears to underperform the network models (based upon interpretation of performance metrics). Depending upon the regression model, CHL *a* concentrations displayed heteroscedasticity and/or modeled residuals signified a condition of non-linearity. In a strict sense, such conditions invalidate the underlying assumptions for linear regression testing (see Reckhow et al., 1990; Osborne, 2002; Osborne and Waters, 2002), providing for a parametric model lacking statistical merit.

The Grey-Box should be considered, at best, an iterative approximation of a conventional ANN. Although the Grey-Box possessed the positive attributes associated with ANNs (i.e. non-linear modeling capabilities, no requirement of a normal probability distribution for data, etc.), a 'less than ideal' 1:1 modeled:measured relationship resulted for the final, non-rotated

cumulative plot. This can be attributed to the partial utilization of candidate predictors (i.e. incorporating eight, rather than 15 variables) and the resulting loss of information encapsulated among auto-correlated variables (refer to Fig. 5D; c.f. Rohani et al., 2004). Rotation and offset corrected the model for instances when the iterative summation plot under- and over-estimated (or conversely, over and under-estimated) data within its lower and upper ranges, respectively, with the final presentation approximating a (desirable) 1:1 modeled:measured relationship. In corroborating the iterative modeling technology with datasets distinct from the Sarasota Bay dataset (e.g. Millie et al., 2006a), the Grey-Box consistently provided greater and lesser prediction accuracies than MLR and holistic ANNs, respectively.

5. Summary and recommended Grey-Box applications

Data sets arising from dynamic ecological systems often require unconventional numerical approaches, necessitating robust and adaptive analyses for data manipulation/minimization, trend analysis, and information synthesis (Wood, 2010; Recknagel, 2011; Michener and Jones, 2012). Because of their robust capability for identifying and reproducing the inherent complexities underlying chaotic, non-linear systems, ANNs have become popular for the statistical-based modeling of ecosystem structure and function. However, ANNs require little (if any) expert knowledge for their application and do not exhibit a declarative knowledge structure; as such, many scientists consider such models to be numerical enigmas.

The holistic ANN and the Grey-Box model outperformed MLR in identifying and reproducing the non-linear, environmental influences upon CHL *a* within Sarasota Bay. The architecture of the Grey-Box provided the benefit of the ANN modeling structure (albeit, at a lesser predictive performance), while utilizing a systematic 'bottom-up' curve-fitting approach. This ultimately afforded a cumulative mathematical formulation of iterative, multivariate nonlinear models. The derivation of an explicit empirical quantitative expression corrected for the lack of declarative knowledge (within conventional ANNs) and allowed the Grey-Box to 'bridge the gap' between white- and black-box models in both mathematical transparency and performance.

The generalization of prediction via the Grey-Box, while utilizing a systematic decrease in predictor variables (in successive iterations) and in more comprehensible manner than that of the ANN, was impressive. However, the derivation of Grey-Box can be cumbersome and manually intensive due to the experimentation required, the generation of output response surfaces, the derivation of iterative weights, and the fitting of mathematical equations to output surfaces. As such, the usage of the Grey-Box technology might be problematic for some applications. Nonetheless, if a certain statistical approach is employed just because it is uncomplicated and/or provides for handling in a simple, exact manner, one runs the risk that the selected methodology disregards or discounts information pertinent to fully understanding the system of interest (Malmgren, 2000). Accordingly, benefits of the declarative knowledge and/or rule sets afforded by the Grey-Box outweigh the aforementioned detriments and advocate its application.

Quantitative knowledge extraction from ANNs modeling biotic responses to environmental forcing plays a vital role in the innovative application of statistical models for ecosystem conceptualization, potentially leading to discoveries of (previously unrecognized) variable relationships and interaction across system- and organismal scales (Browne et al., 2003; Millie et al., 2011; Recknagel, 2011; Michener and Jones, 2012). It is imagined that the Grey-Box model will fuel a greater acceptance for, and routine usage of ANNs within studies of ecological assessment and problem solving. The Grey-Box derivation particularly is pertinent to the development of data-driven models predicting a species' presence–absence, abundance dynamics, and/or distribution based upon system-specific abiotic/biotic, geographic and/or historic influences (akin to ecological niche modeling, Peterson, 2001, 2006; Peterson and Kluza, 2005; Carrick, 2011). The quantitative, declarative knowledge provided by the Grey-Box could provide time-specific predictions of a species occurrence, with response surfaces affording comprehensible projections of species presence/quantities within the data boundaries of autecological and/or synecological predictors. Within this context, Grey-Box formulations are relevant to applications attempting to identify biotic response(s) to environmental stress and disturbance thresholds (see Clements and Rohr, 2009; Baker and King, 2010). Brenden et al. (2008) noted that accuracies in identifying such thresholds are affected by multiple factors and, in order to circumvent difficulties in interpretation of results, advocated the use of robust, quantitative approaches that included plotting and visualization of data. The Grey-Box approach accomplishes this.

Additionally, Grey-Box derivations appear advantageous for coastal monitoring programs where the recent, increased reliance upon autonomous data acquisition has resulted in the generation of copious amounts of auto-correlated data that users must synthesize and ultimately interpret (see Paerl et al., 2005; Millie et al., 2006a; Reed et al., 2010). Initially, the Grey-Box could afford the identification and minimization of pertinent predictor variables (for a specific modeled response), with qualitative/quantitative functionalities generated for single (or multiple) locale(s). Derived 'definitions' of biota-environmental relationships from specific locales then could be incorporated into stand-alone mechanistic models projecting ecological structure and/or estimating deviations from predictability over larger geographic scales (after Millie et al., 2006b, 2011).

Acknowledgements

Funding for this research was provided by the Florida Department of Environmental Protection, Florida Coastal Management Program (through grants from the National Oceanic and Atmospheric Administration [NOAA] Office of Ocean and Coastal Resource Management under the Coastal Zone Management Act of 1972, as amended, Award #s NA10NOS4190178 and NA11NOS4190073) and by the *Oceans and Human Health Initiative* of NOAA's Office of Global Programs, Center for Sponsored Coastal Ocean Research. Reference to proprietary names are necessary to report factually on available data; however, Palm Island Enviro-Informatics LLC, Loyola University New Orleans, the State of Florida, the Ohio University, Central Michigan University, and NOAA neither guarantee nor warrant the standard of a product and imply no approval of a product to the exclusion of others that may be suitable. The statements, findings, and recommendations expressed herein are those of the authors alone. This work is contribution #1616 of NOAA's Great Lakes Environmental Research Laboratory and contribution #19 of the Institute for Great Lakes Research, Central Michigan University.

References

Austin, M.P., 2002. Spatial prediction of species distribution: an interface between ecological theory and statistical modeling. Ecol. Model. 157, 101–118.

Bachmann, R.W., Hoyer, M.V., Canfield Jr., D.E., 2001. Evaluation of recent limnological changes at Lake Apopka. Hydrobiologia 448, 19–26.

Bachmann, R.W., Jones, B.L., Fox, D.D., Hoyer, M., Bull, L.A., Canfield Jr., D.E., 1996. Relations between trophic state indicators and fish in Florida (USA) lakes. Can. J. Fish. Aquat. Sci. 53, 842–855.

Baker, M.E., King, R.S., 2010. A new method for detecting and interpreting biodiversity and ecological community thresholds. Methods Ecol. Evol. 1, 25–37.
Barciela, R.M., Garcia, E., Fernández, E., 1999. Modelling primary production in a coastal embayment affected by upwelling using ecosystem models and artificial neural networks. Ecol. Model. 120, 199–211.
Brenden, T.O., Wang, L., Zhenming, S., 2008. Quantitative identification of disturbance thresholds in support of aquatic resource management. Environ. Manage. 42, 821–832.
Browne, A., Hudson, B., Whitley, D., Ford, M., Picton, P., Kazemian, H., 2003. Knowledge extraction from neural networks. In: Proc. 29th Ann. Conf. IEEE Soc., Roanoke, Virginia, pp. 1909–1913.
Carrick, H.J., 2011. Niche modeling and predictions of algal blooms in aquatic ecosystems. J. Phycol. 47, 709–713.
Cattaneo, A., 1987. Periphyton in lakes of different trophy. Can. J. Fish. Aquat. Sci. 44, 296–303.
Chan, W.S., Recknagel, F., Cao, H., Park, H.-D., 2007. Elucidation and short-term forecasting of microcystin concentrations in Lake Suwa (Japan) by means of artificial neural networks and evolutionary algorithms. Wat. Res. 41, 2247–2255.
Clements, W.H., Rohr, J.R., 2009. Community responses to contaminants: using basic ecological principles to predict ecotoxicological effects. Environ. Toxicol. Chem. 28, 1789–1800.
Dodds, W.K., Smith, V.H., Lohman, K., 2002. Erratum: Nitrogen and phosphorus relationships to benthic algal biomass in temperate streams. Can. J. Fish. Aquat. Sci. 59, 865–874.
Dodds, W.K., Smith, V.H., Lohman, K., 2006. Nitrogen and phosphorus relationships to benthic algal biomass in temperate streams. Can. J. Fish. Aquat. Sci. 63, 1190–1191.
Florida Department of Environmental Protection (FDEP), 2006. Water Quality Assessment Report: Sarasota Bay and Peace and Myakka Rivers. Division of Water Resource Management, Bureau of Watershed Management, Tallahassee, Florida.
Gevery, M., Dimopoulos, I., Lek, S., 2003. Review and comparison of methods to study the contribution of variables in artificial network models. Ecol. Model. 160, 249–264.
Gilbert, P.M., Harrision, J., Heil, C., Seitzinger, S., 2006. Escalating worldwide use of urea – a global change contributing to coastal eutrophication. Biogeochemistry 77, 441–463.
Gill, P., Murray, W., Wright, M., 1981. Practical Optimization. Academic Press, London.
Goh, A.T.C., 1995. Back-propagation neural networks for modeling complex systems. Artif. Intell. Eng. 9, 143–151.
Gonzalez, S., 2000. Neural Networks for macroeconomic forecasting: a complimentary approach to linear regression models. Canadian Department of Finance Working Paper No. 2000-07, Ottawa, Ont., Canada.
Gurbuz, H., Kirvak, E., Soyupak, S., Yerli, S., 2003. Predicting dominant phytoplankton quantities in a reservoir by using neural networks. Hydrobiologia 504, 133–141.
Heffernan, J.B., Liebowitz, D.M., Frazer, T.K., Evans, J.M., Cohen, M.J., 2010. Algal blooms and the nitrogen-enrichment hypothesis in Florida springs: evidence, alternatives, and adaptive management. Ecol. Appl. 20, 816–829.
Horkik, K., Stinchcombe, White, M., 1989. Multilayer feedforward networks are universal approximators. Neural Networks 2, 359–366.
Hu, Y.H., Hwang, J.-N., 2001. Introduction of neural networks for signal processing. In: Hu, Y.H., Hwang, J.-N. (Eds.), Handbook of Neural Network Signal Processing. CC Press, Boca Raton, Florida, pp. 1–30.
Jeong, K.-S., Recknagel, F., Joo, G.-J., 2003. Prediction and elucidation of population dynamics of the blue-green algae *Microcystis aeruginosa* and the diatom *Stephanodiscus hantzschii* in the Nakdong River-Reservoir system (South Korea) by a recurrent artificial neural network. In: Recknagel, F. (Ed.), Ecological Informatics; Understanding Ecology by Biologically-Inspired Computation. Springer-Verlag, Berlin, pp. 195–213.
Johannet, A., Vayssade, B., Bertin, D., 2007. Neural networks: from black box toward transparent box application to evapotranspiration modeling. Proc. World Acad. Sci. Eng. Technol. 24, 162–169.
Karul, C., Soyupak, S., Cilesiz, A., Akbay, N., Germen, E., 2000. Case studies on the use of neural networks in eutrophication modeling. Ecol. Model. 134, 145–152.
Jeong, K.-S., Kim, D.-K., Jung, J.-M., Kim, M.-C., Joob, G.-J., 2008. Non-linear autoregressive modelling by Temporal Recurrent Neural Networks for the prediction of freshwater phytoplankton dynamics. Ecol. Model. 211, 292–300.
Lasdon, L., Waren, D., Jain, A., Ratner, M., 1978. Design and testing of a generalized reduced gradient code for nonlinear programing. ACM Trans. Math. Soft. 4, 34–49.
Lee, J.H.W., Huang, Y., Dickman, M., Jayawardena, A.W., 2003. Neural network modeling of coastal algal blooms. Ecol. Model. 159, 179–201.
Lek, S., Guegan, J., 1999. Artificial neural networks as a tool in ecological modeling, an introduction. Ecol. Model. 120, 65–73.
Maier, H.R., Dandy, G.C., Burch, M.D., 1998. Use of artificial neural networks for modeling cyanobacteria *Anabaena* spp. in the River Murray, South Australia. Ecol. Model. 105, 257–272.
Malmgren, H., 2000. Artificial neural networks in medicine and biology; a philosophical introduction. Opening lecture at the Artificial Neural Networks in Medicine and Biology (ANNIMAB)-1 conference, Göteborg, Sweden, May 13–16. ISSN: 1652-0459. Available at: http://gupea.ub.gu.se/handle/2077/19466.
Michener, W.K., Jones, M.B., 2012. Ecoinformatics: supporting ecology as a data-intensive science. Trends Ecol. Evol. 27, 85–93.
Millie, D.F., Fahnenstiel, G.L., Weckman, G.R., Klarer, D.M., Dyble Bressie, J., Vanderploeg, H.A., Fishman, D., 2011. An 'enviro-informatic' assessment of Saginaw Bay (Lake Huron USA) phytoplankton: characterization and modeling of *Microcystis* (Cyanophyta). J. Phycol. 47, 714–730.
Millie, D.F., Pigg, R.L., Fahnenstiel, G.L., Carrick, H.J., 2010. Algal chlorophylls: a synopsis of analytical methodologies. In: American Water Works Association, Manual M57, Algae. American Water Works Association, Denver, Colorado, pp. 93–122.
Millie, D.F., Fahnenstiel, G.L., Dyble, J., Pigg, R., Rediske, R., Litaker, R.W., Tester, P.A., 2009. Late-summer phytoplankton in western Lake Erie (Laurentian Great Lakes): bloom distributions, environmental influences, and toxicity. Aquat. Ecol. 43, 915–934.
Millie, D.F., Weckman, G.R., Paerl, H.W., Pinckney, J.L., Bendis, B.J., Pigg, R.J., Fahnenstiel, G.L., 2006a. Neural network modeling of estuarine indicators: hindcasting phytoplankton biomass and net ecosystem production in the Neuse (North Carolina) and Trout (Florida) Rivers. Ecol. Ind. 6, 589–608.
Millie, D.F., Pigg, R., Tester, P.A., Dyble, J., Litaker, R.W., Carrick, H.J., Fahnenstiel, G.L., 2006b. Modeling phytoplankton abundance in Saginaw Bay, Lake Huron: using artificial neural networks to discern functional influence of environmental variables and relevance to a Great Lakes Observing System. J. Phycol. 42, 336–349.
Millie, D.F., Carrick, H.J., Doerong, P.H., Steidinger, K.A., 2004. Intra-annual variability of water quality and phytoplankton within the St. Lucie River Estuary (Florida, USA): a quantitative perspective. Estuar. Coast. Shelf Sci. 61, 137–149.
Moré, J.J., 1978. The Levenberg-Marquardt algorithm: implementation and theory. Lect. Notes Math. 630, 105–116.
Murray, K., Conner, M.M., 2009. Methods to quantify variable importance: implications for the analysis of noisy ecological data. Ecology 90, 348–355.
Oksanen, J., Minchinb, P.R., 2002. Continuum theory revisited: what shape are species responses along ecological gradients? Ecol. Model. 157, 119–129.
Olden, J.D., 2000. An artificial neural network approach for studying phytoplankton succession. Hydrobiologia 436, 131–143.
Olden, J.D., Jackson, D.A., 2002. Illuminating the "black box": understanding variable contributions in artificial neural net- works. Ecol. Model. 154, 135–150.
Olden, J.D., Joy, A.K., Death, R.G., 2004. An accurate comparison of methods for quantifying variable importance in artificial neural networks using simulated data. Ecol. Model. 178, 389–397.
Osborne, J., Waters, E., 2002. Four assumptions of multiple regression that researchers should always test. Available at: Pract. Asses. Res. Eval. 8 (2) http://PAREonline.net/getvn.asp?v=8&n=2
Osborne, J., 2002. Notes on the use of data transformations. Available at: Pract. Asses. Res. Eval. 8 (6) http://PAREonline.net/getvn.asp?v=8&n=6
Oussar, Y., Dreyfus, G., 2001. How to be a gray box: dynamic semi-physical modeling. Neural Net. 14, 1161–1172.
Paerl, H.W., 1988. Nuisance phytoplankton blooms in coastal, estuarine, and inland waters. Limnol. Oceanogr. 33, 823–847.
Paerl, H.W., Dyble, J., Pinckney, J.L., Valdes, L.M., Millie, D.F., Moisander, P.H., Morris, J.T., Bendis, B., Piehler, M.F., 2005. Using microalgal indicators to assess human and climatically-induced ecological change in estuaries. In: Bortone, S.A. (Ed.), Estuarine Indicators. CRC Press, Boca Raton, FL, pp. 145–174.
Paerl, H.W., Pinckney, J.L., Fear, J.M., Peierls, B.L., 1998. Eco-system responses to internal and watershed organic matter loading: consequences for hypoxia in the eutrophying Neuse River Estuary, North Carolina, USA. Mar. Ecol. Prog. Ser. 166, 17–25.
Peck, M.S., Leffler, A.J., Flint, S.D., Rywl, R.J., 2003. How much variance is explained by ecologists? Additional perspectives. Oecologia 137, 161–170.
Peterson, A.T., 2001. Predicting species' geographic distributions based on ecological niche modeling. Condor 103, 599–605.
Peterson, A.T., 2006. Uses and requirements of ecological niche models and related distributional models. Biodiv. Inform. 3, 59–72.
Peterson, A.T., Kluza, D.A., 2005. Ecological niche modeling as a new paradigm for large-scale investigations of diversity and distribution of birds. U. S. Department of Agriculture, Forest Service Gen. Tech. Rep. PSW-GTR-191.
Principe, J.C., Euliano, N.R., Lefebrve, W.C., 2000. Neural and Adaptive Systems: Fundamentals Through Simulation. John Wiley and Sons Inc., New York.
Reckhow, K.H., Clements, J.T., Dodd, R.C., 1990. Statistical evaluation of mechanistic water-quality models. J. Environ. Eng. 116, 250–268.
Recknagel, F., 2011. Ecological informatics: a discipline in the making. Ecol. Inform. 6, 1–3.
Recknagel, F., French, M., Harkonen, P., Yabunaka, K.-I., 1997. Artificial neural network approach for modeling and prediction of algal blooms. Ecol. Model. 96, 11–28.
Reed, R.E., Burkholder, J.M., Allen, E.H., 2010. Current online monitoring technology for surveillance of algal blooms, potential toxicity, and physical–chemical structure in rivers, reservoirs, and lakes. In: American Water Works Association, Manual M57, Algae. American Water Works Association, Denver, Colorado, pp. 1–24.
Rohani, P., Miramontes, O., Keeling, M.J., 2004. The colour of noise in short ecological time series data. Math. Med. Biol. 21, 63–72.
Saito, K., Nakano, R., 2002. Extracting regression rules from neural networks. Neural Net. 15, 1279–1288.
Saltelli, A., Tarantola, S., Compolongo, F., Ratto, M., 2004. Sensitivity Analysis in Practice: A Guide to Assessing Scientific Models. John Wiley & Sons, Ltd, West Sussex, England.
Sarnelle, O., 1992. Nutrient enrichment and grazer effects on phytoplankton in lakes. Ecology 74, 551–560.
Scardi, M., 2001. Advances in neural network modeling of phytoplankton primary production. Ecol. Model. 146, 33–45.
Scardi, M., Harding Jr., L.W., 1999. Developing an empirical model of phytoplankton primary production: a neural network case study. Ecol. Model. 120, 213–223.

Stow, C.A., Roessler, C., Borsuk, M.E., Bowen, J.D., Reckhow, K.H., 2003. Comparison of estuarine water quality models for total maximum daily load development in Neuse River Estuary. J. Wat. Resour. Plan. Manag. 129, 307–314.

Sugihara, G., Grenfell, B., May, R.M., 1990. Distinguishing error from chaos in ecological time series. Phil. Trans. R. Soc. Lond. B 330, 235–251.

Teles, L.O., Vasconcelos, V., Pereira, E., Saker, M., 2006. Time series forecasting of cyanobacteria blooms in the Crestuma Reservoir (Douro River, Portugal) using Artificial Neural Networks. Environ. Manag. 38, 227–237.

Weckman, G.R., Millie, D.F., Ghai, V., Ganduri, C., 2005. A comparison of knowledge extraction techniques from an artificial neural network in ecological monitoring. In: Dagli, C.H., Buczak, A.L., Enke, D.L., Embrechts, M.J., Ersoy, O. (Eds.), Intelligent Engineering Systems Through Artificial Neural Networks. Smart Engineering System Design, Neural Networks, Evolutionary Programming, and Artificial Life, vol. 15. ASME Press, New York, pp. 761–766.

Weckman, G.R., Millie, D.F., Ganduri, C., Rangwala, M., Young, W., Fahnenstiel, G.L., 2009. Knowledge extraction from the neural 'black box' in ecological monitoring. J. Indust. Syst. Eng. 3, 38–55.

Wood, S.N., 2010. Statistical inference for noisy nonlinear ecological dynamic systems. Nature 466, 1102–1104.

Yeung, D., Cloete, I., Shi, D., Ng, W., 2010. Sensitivity Analysis for Neural Networks, Neural Computing Series. Springer-Verlag, Berlin/Heidelberg.

Young, W., Weckman, G., 2009. Using a heuristic approach to derive a grey-box model through an Artificial Neural Network knowledge extraction technique. J. Neural Comput. Appl. 19, 353–366.